Fully automated hematoma expansion prediction from non-contrast computed tomography in spontaneous intracerebral hemorrhage patients

Natasha Ironside, MBChB[1]; Kareem El Naamani, MD[2]; Tanvir Rizvi, MD[3]; Mohammed Shifat E-Rabbi, PhD[4]; Shinjini Kundu, MD, PhD[5]; Andrea Becceril-Gaitan, MD[6]; Ching-Jen Chen, MD[6]; Stephan Mayer, MD[7]; E. Sander Connolly, MD[8]; Gustavo Rohde, PhD[4,9] on behalf of the VISTA-ICH collaboration*

[1]*Department of Neurological Surgery, University of Virginia Health System, Charlottesville, VA*
[2]*Department of Neurological Surgery, Thomas Jefferson University, Philadelphia, PA*
[3]*Department of Radiology, University of Virginia Health System, Charlottesville, VA*
[4]*Department of Biomedical Engineering, University of Virginia, Charlottesville, VA*
[5]*Department of Radiology, The Johns Hopkins Hospital, Baltimore, MD*
[6]*Department of Neurosurgery, The University of Texas Health Science Center, Houston, TX*
[7]*Department of Neurology, Westchester Medical Center, Westchester, NY*
[8] *Department of Neurological Surgery, Vagelos College of Physicians and Surgeons, Columbia University, New York, NY*
[9]*Department of Electrical and Computer Engineering, University of Virginia, Charlottesville, VA*

***VISTA-ICH Steering Committee:** DF Hanley (Chair), K Butcher, S Davis, B Gregson, KR Lees, P Lyden, S Mayer, K Muir, and T Steiner

Running title: Fully automated hematoma expansion prediction after ICH

Key words: intracerebral hemorrhage; hematoma expansion; artificial intelligence; automated prediction; transport-based morphometry; computed tomography; machine learning

Figures/Tables: Figures: 5, Tables : 1

Correspondance:
Natasha Ironside, MBChB
Department of Neurological Surgery
University of Virginia Health System
1215 Lee Street
Charlottesville
Virginia 22903
USA
+14349240000
ni8vb@uvahealth.org

Abstract

Background

Hematoma expansion is an independent predictor of poor neurological outcome after spontaneous intracerebral hemorrhage (ICH), and a promising quantifiable and modifiable therapeutic target. Practical tools to identify patients at risk of hematoma expansion are lacking, limiting early preventative intervention. We hypothesized that three-dimensional transport-based morphometry (3D-TBM), could automatically predict future hematoma expansion from non-contrast computed tomography (NCCT) images at the time of hospital presentation.

Methods

One hundred and seventy spontaneous ICH patients enrolled in the multi-center international Virtual International Trials of Stroke Archive (VISTA-ICH), were separated into training (60%) and testing (40%) cohorts for model derivation and validation, respectively. A unique transport-based representation was produced from each presentation NCCT hematoma image for statistical analysis. The 3D-TBM model was interrogated to visualize the physical hematoma characteristics predictive of future expansion.

Results

3D-TBM outperformed each of the existing clinician-based BAT, Brain, Heavn, NAG and 10-point NCCT hematoma expansion prediction scores in the testing dataset. 3D-TBM adjusted for location and clinical information predicted hematoma expansion in the testing dataset with an area under the receiver operating characteristic curve (AUROC) of 0.698 (95% CI 0.695-0.702), while the AUROC for the best performing clinician method, the Heavn score, was 0.663 (95%

CI 0.660–0.666). The predominant hematoma characteristics predicting future expansion were larger size, textural heterogeneity, shape irregularity and peripheral intensity distribution.

Discussion

We present a quantitative method that outperformed clinicians and permitted visualization of the morphometric features for predicting hematoma expansion from NCCT in ICH patients. Our study contributes insight into the underlying mechanisms driving hematoma expansion and suggests that it can be identified at a reversible stage.

Introduction

Within hours of spontaneous intracerebral hemorrhage (ICH) onset, hematoma expansion contributes to mass effect and injury to surrounding brain.[1-3] It is a potentially preventable predictor of poor neurological outcome and mortality.[1,2] However, treatment strategies to prevent hematoma expansion have been limited by their inability to select high-risk patients efficiently an accurately.[4] NCCT radiographic markers of expansion are rapidly accessible, easily acquired, and broadly implementable.[5-8] Published scoring systems based on expert clinician NCCT interpretation to predict expansion risk have had limited impact on clinical and research decision-making to date.[2,6-9] This is because they were predominantly derived from retrospective single-center observational data, required medical knowledge for implementation, and lacked connection to the underlying disease pathophysiology.[4,8,9] Their need for NCCT interpretation leads to Recent promising results demonstrating a neurological benefit to ICH surgical evacuation motivates new approaches to enable early detection of hematoma expansion and reduce time-to-intervention in future ICH trial designs.[4,9,10]

In this study, we hypothesized that hematoma expansion could be reliably predicted from NCCT scans obtained at the time of hospital presentation. We developed a fully automated and quantitative method using the mathematics of optimal mass transport.[11-13] We considered normalized Hounsfield Unit (HU) pixel intensity values as relative measurements of blood density and assumed that hematoma expansion occurs as a continuous process of red blood cell movement under the effect of unknown biological and physical influences.[13] This assumption permits the 3D transport-based morphometry (TBM) technique to model the relative intensity of each pixel in a segmented NCCT hematoma image with reference to a template, generating a

three-dimensional representation of the entire information content within the image.[14-17,] Using segmented time-series NCCT scans from the ICH section of the multicenter, international Virtual International Trials in Stroke Archive (VISTA-ICH), we applied our 3D-TBM model to investigate relationships between NCCT morphometric features and hematoma expansion.[17,18]

Our objectives were to (1) predict hematoma expansion automatically and accurately in ICH patients and (2) directly visualize the image characteristics of the hematoma responsible for future expansion.

Methods

Study Population

This post-hoc analysis of spontaneous ICH patients from VISTA was prepared according to the Standards for Reporting Diagnostic accuracy studies (STARD) guideline.[18] VISTA is an international collaborative pooled repository of anonymized patient data from randomized clinical trials. Inclusion criteria were: (1) age ≥18 years, (2) enrolment in neutral non-surgical ICH trials, (3) presentation with CT-proven ICH within 4 hours after symptom onset, (4) at least one subsequent CT scan at 24±6 hours after the initial scan, (5) available baseline clinical and laboratory data, (6) supratentorial location, and (7) initial volume ≥7 mL. Initial volume was set to distinguish microbleeds from the range of volumes associated with hematoma expansion.[33] Exclusion criteria were: (1) primary intraventricular hemorrhage (IVH), and (2) ICH related to suspected secondary causes.

Standard Protocols, Approvals, Registrations, and Patient Consents

This study uses data that were not collected specifically for this study and no one on our study

team had access to the subject identifiers linked to the specimens or data. Therefore, this study is not considered human subjects research. Because it is not considered human subjects research, an institutional review board exemption was not required to conduct this study.

Clinical information

Baseline clinical and demographic variables are detailed in the **Online-only supplement.** To account for inter-patient differences in the time interval from symptom onset to presentation NCCT, hematoma growth rate was defined as: time from symptom onset to first NCCT÷presentation hematoma volume (min/mL).

Hematoma segmentation

The de-identified NCCT scans at presentation and 24±6 hours after the initial scan were transferred in Digital Imaging and Communications in Medicine (DICOM) format to a central workstation. Hematoma regions were segmented by two independent raters who were blinded to outcomes information (T.R., board-certified neuroradiologist with 20 years of experience; K.E.N., neurosurgeon in-training), according to our previously described manual method, described in detail in the **Online-only supplement**.[32]

NCCT hematoma features

Established NCCT features associated with hematoma expansion were ranked by two independent raters who were blinded to outcomes information (A.B-G, neurosurgeon in-training; K.E.N., neurosurgeon in-training), as described in the **Online-only supplement**. These features were used in combination with clinical information to compute the BAT,

BRAIN, HEAVN, NAG and 10-point scores.[6,21-24]

NCCT scan preprocessing

NCCT data was pre-processed according to a standard protocol, described in the **Online-only supplement**.

Hematoma volumetry

After NCCT scan preprocessing, ICH volumes at presentation and 24±6 hours were measured by multiplying the number of voxels (volumetric pixels) in the segmented hematoma region by the volume of each voxel (1x1x1 mm).

3D transport-based morphometry

The optimal mass transport problem seeks the most efficient way of transforming one distribution of mass to another, by minimizing a cost function.[34] Normalizing each image so that the pixel intensities sum to the same total mass allows the images to be interpreted as probability measures. In this context, mass is represented as the image intensity.[14] A description of the continuous linear optimal transportation problem and its solution is in the **Online-only supplement**.

Template image

The linear embedding is calculated with respect to an intrinsic mean template image I_0. The intrinsic mean template image I_0 represents the average hematoma appearance for the dataset. Generation of the template image is described in the **Online-only supplement**.

Supervised learning

Solving the continuous optimal transportation problem results in a unique linearly embedded 3D mass preserving (MP) map. We obtained the MP map for the segmented presentation NCCT hematoma of each patient. These data were shuffled at random and separated into independent training (60%) and testing (40%) cohorts for subsequent statistical analyses. To minimize bias in data sampling for robust statistical analysis, this process was repeated 1000 times to generate 1000 different testing and training splits. The dataset composition is described further in the **Online-only supplement**. Statistical analyses and data visualization were performed independently on each of the 1000 cross-validation samples, and the mean results with corresponding 95% confidence intervals are presented. The *p*-values were averaged using the Fisher's method. Statistical significance was defined as $p<0.05$. The code used for model derivation is available as an open-source package.[35]

Outcomes

Outcomes were (1) significant hematoma expansion, defined as ≥ 6mL increase in hematoma volume between the presentation and 24±6-hour NCCT scans, and (2) hematoma growth, defined as absolute hematoma volume (mL) increase between the presentation and 24±6 hour NCCT scans. Absolute hematoma volume increase (mL) was chosen for its reduced susceptibility to the effect of the size of the initial hematoma and stronger association with clinical outcome, than relative volume change (%). Significant hematoma expansion was set at 6 mL to reflect the threshold most used by established hematoma expansion prediction methods and in ICH clinical outcomes studies.[1,4,8] For the prediction of neurological outcome, lower hematoma expansion

thresholds have been found to provide improved sensitivity at the expense of specificity, while higher thresholds provide improved specificity at the expense of sensitivity.[2,4]

Principal Components Analysis

Because the dimensionality of the hematoma image features in transport space was much higher than the number of data samples, we utilized the principal components analysis (PCA) for dimensionality reduction.[14,17] PCA is described in detail in the **Online-only supplement**. PCA eliminated the components with little contribution to the overall variance, the likelihood of overfitting and maintained separation of the training and testing datasets.

Penalized Linear Discriminant Analysis

To assess the relationship between presentation NCCT hematoma image features and 24-hour hematoma expansion, we used the penalized linear discriminant analysis (pLDA) method, described in the **Online-only supplement**.[15] The independent *t*-test was used to assess the separation between the expansion and no expansion groups in the testing dataset.

Hematoma Expansion Prediction

The training dataset projected onto the top pLDA direction, w^0, was used to train a classifier which assigned patients to the expansion or no expansion groups. The trained classifier was applied to the testing dataset to predict expansion and area under the receiver operator characteristic curve (AUROC) analyses evaluated the model's performance. Classification accuracy was assessed using sensitivity, specificity, positive predictive value (PPV) and negative predictive value (NPV).

Hematoma Growth Prediction

The canonical correlation analysis (CCA) method determined the relationship between presentation NCCT hematoma image features and 24-hour change in hematoma volume (mL), described in detail in the **Online-only supplement**.[14,17] The Pearson's correlation coefficient (CC) was used to assess the strength of the relationship between the testing dataset and 24-hour hematoma volume change (mL).

Effect of hematoma location

To evaluate the independent effect of hematoma location on expansion, we defined location as the *x*, *y* and *z* co-ordinates of the center of each presentation NCCT hematoma image and used covariance matrices to represent the initial hematoma location. The pLDA method assessed the effect of location for predicting significant expansion.

Location, Volume and Clinical Information-Adjusted Hematoma Expansion and Hematoma Growth Prediction Models

As TBM is not invariant to translation or scaling, we hypothesized that rendering the MP mappings volume and location invariant and adjusting for location, initial volume and clinical information would improve the model's overall performance. To test this, we translated and scaled each presentation NCCT hematoma image according to its location and volume prior to optimal transportation. This is described in detail in the **Online-only supplement**. We then generated multivariable TBM models for predicting 24-hour hematoma expansion and hematoma growth. Their performance was assessed using abovementioned statistical methods.

Visualization

The continuous linear optimal transportation approach is generative and any point in the transport space can be visualized by inverting its linear embedding. This is described in the **Online-only supplement**. After statistical analyses, we inverted the TBM model to visualize presentation NCCT hematoma image features associated with greater likelihood of 24-hour expansion and growth. We also translated the location model to visualize directions that predicted significant expansion.

Hematoma morphometric features of expansion

Visual inspection of the TBM model identified NCCT hematoma image features discriminating 24-hour expansion. The significance of these predictors of hematoma expansion was retrospectively tested using the presentation NCCT hematoma image data. The independent *t*-test was used to assess the separation between the expansion and no expansion groups and AUROC analyses evaluated the predictive accuracy of each feature in the testing dataset with comparison to the TBM model. This is described in the **Online-only supplement**.

Comparison to alternate NCCT prediction scores

The performance of the TBM model in predicting 24-hour expansion was assessed against the BAT, BRAIN, HEAVN, NAG and 10-point clinician based scores ranked by two independent raters who were blinded to outcomes information (A.B-G, neurosurgeon in-training; K.E.N., neurosurgeon in-training), by comparing the AUROC for each model in the testing dataset. The strength of the relationship between increasing score and greater 24-hour hematoma growth (mL) was evaluated by comparing the Pearson's correlation co-efficient for each model in the testing

dataset.

Results

Dataset composition

Of the 265 spontaneous ICH patients in the VISTA repository with available presentation NCCT scans, 95 were excluded (**eFigure 1**). The remaining 170 patients (mean (SD) age 64.08 (12.45) years; 37.6% (n=64) female), comprised the dataset. The mean (SD) and median [IQR] hematoma volumes at presentation were 31.31 (24.06) and 25 [14- 39] mL, respectively. The mean (SD) and median [IQR] hematoma volumes at 24±6 hours were 39.56 (34.42) and 28 [14-54] mL, respectively. Hematoma expansion was present in 32.9% (n=56) patients. Intraventricular extension at presentation was present in 33.5% (n=57) patients. Comparisons of baseline demographic and clinical characteristics between the expansion and no expansion groups are presented in **Table1**.

Data preprocessing

The NCCT preprocessing and segmentation is shown in **Figure 1A-I**. Comparisons of the segmented presentation NCCT hematoma images did not identify a visually discernible difference between the expansion (**Figure 1J)** and no expansion groups (**Figure 1K)**. The intrinsic mean template $I_{0\mu}$ for the linear optimal transportation framework is shown for each dataset in **eFigure 2**.

24-hour hematoma expansion prediction

In the final TBM model adjusted for location and clinical information, there was a significant right shift in the mean probability distribution of the hematoma features projected onto the most discriminant direction in transport space w^0 for the expansion group, when compared to the no expansion group, in the testing dataset ($p<0.0001$) **(Figure 2A).** The mean AUROC for the classifier distinguishing between the expansion and no expansion groups was 0.698 [0.695-0.702] in the testing (**Figure 2B**) dataset. In the testing dataset, the mean accuracy, sensitivity and specificity were 67.9% [67.6-68.2%], 51.0% [50.5-51.6%], and 77.6% [77.3-77.9%], respectively. The inverse transformations of the hematoma features projected onto w^0 are shown in **Figures 2C and 2D**, plotted in units of standard deviations (SD) of the pixel intensity distribution along w^0. Upon visual inspection, the features that discriminated expansion were larger size, elongated shape, peripheral intensity distribution, and textural heterogeneity. Stepwise results for the trained expansion prediction models are presented in the **Online-only supplement; eFigures 3, 4, 5, 6**.

24-hour hematoma growth prediction

In the final TBM model adjusted for location and clinical information, the mean CC for the most correlated direction in transport space w_{corr} between presentation NCCT hematoma features and 24-hour hematoma growth was 0.278 [0.271–0.285]; $p<0.0001$ in the testing **(Figure 3A)** dataset. The inverse transformations of the presentation hematoma features projected onto w_{corr} are shown in **Figure 3B and 3C**, plotted in units of SD of the pixel intensity distribution along w_{corr}. Upon visual inspection, the features associated with more growth were larger size, peripheral intensity distribution and elongated shape. Stepwise results for the preliminary trained growth prediction models are presented in the **Online-only**

supplement; eFigures 7 and 8.

Effects of location

There was a significant right shift in the mean probability distribution of the hematoma location projected onto the most discriminant direction in transport space for the expansion group, when compared to the no expansion group, in both the testing ($p<0.0001$) **(eFigure 9C)** and training ($p<0.0001$) datasets **(eFigure 9D)**. The mean AUROC for the most discriminant hematoma location that separated the expansion and no expansion groups was 0.600 [0.597-0.603] in the testing **(eFigure 9A)** dataset. The inverse transformations plotted in unit vectors along the most discriminant direction in the axial, coronal and sagittal planes showed hematomas associated with greater likelihood of expansion to be oriented posteriorly, inferiorly and medially towards the thalamus, posterior limb of the internal capsule and the atrium of the lateral ventricle **(Figure 4)**.

Image features

There was a significant separation in the distributions of hematoma size ($p<0.0001$), textural heterogeneity ($p<0.0001$), elongated shape ($p<0.0001$) and peripheral intensity distribution ($p<0.0001$) between the expansion and no expansion groups **(eFigures 10 and 11)**. AUROC analyses found the final TBM model adjusted for location and clinical information to outperform each of the aforementioned features in predicting 24-hour hematoma expansion in both the testing and training datasets **(eFigure 12)**.

Comparison to clinician based hematoma expansion prediction methods

The mean AUROC in predicting 24-hour hematoma expansion was 0.660 [0.656-0.663] for BAT, 0.623 [0.620–0.627] for BRAIN, 0.663 [0.660–0.666] for HEAVN, 0.578 [0.575–0.581] for NAG, and 0.563 [0.561–0.567] for 10-point scores in the testing dataset. The mean accuracy in predicting 24-hour hematoma expansion was 63.2% [62.8–63.6%] for BAT, 59.1% [58.5–59.7%] for BRAIN, 62.9% [62.5–63.3%] for HEAVN, 51.1% [50.4–51.7%] for NAG, and 63.2% [62.8–63.7%] for 10-point scores in the testing dataset. The final TBM model outperformed each score for predicting 24-hour hematoma expansion in both the testing **(Figure 5A)** and training **(Figure 5B)** datasets. The mean CC for higher score and 24-hour hematoma growth was 0.220 [0.215-0.224] for BAT, 0.109 [0.104-0.114] for BRAIN, 0.207 [0.201-0.212] for HEAVN, 0.143 [0.137-0.148] for NAG, and 0.096 [0.089-0.102] for 10-point score, in the testing dataset. The final TBM model outperformed each score in predicting 24-hour hematoma growth in both the testing and training datasets **(eFigure 13)**.

Discussion

Hematoma expansion is an established independent predictor of poor neurological outcome and mortality that can potentially be prevented with early surgical ICH evacuation or hemostatic therapies.[3,9,19,20] The recently published early minimally invasive removal of intracerebral hemorrhage (ENRICH) randomized trial is the first to demonstrate improved neurological outcomes with surgical removal of the hematoma among patients treated within 24 hours after ICH symptom onset.[10] However, efficient methods to identify patients at risk for hematoma expansion are lacking.[8] In this study of 170 ICH patients from VISTA, our 3D-TBM model adjusted for location and clinical information predicted hematoma expansion from presentation NCCT with an AUC of 0.7 in the testing dataset. Our 3D-TBM model outperformed established

NCCT hematoma expansion prediction methods scored by clinicians, that comprised both image feature and clinical information.[6,21-24] Our results indicate that 3D-TBM is a better prognostic tool for predicting hematoma expansion than clinicians. Our method affords offers advantages of both quantitative and automated analyses. This obviates the need for clinician input to discriminate image features, accounts for limitations of inter-rater variability, and permits grading of hematoma morphometric features to estimate future hematoma volume on an individual patient basis.

Visualization of the image features identified by our 3D-TBM model further represents a key advance over alternative machine learning approaches as it permits hypothesis-generation for the mechanisms driving hematoma expansion.[12] For example, our observation of preferential intensity distribution towards the hematoma periphery suggests that expansion may occur via a continuous process. This can direct future investigations toward understanding injury pathways after spontaneous ICH and designing preventative strategies to limit expansion. While the affected location may harbor characteristic structural properties that facilitate expansion, there is conflicting evidence regarding location(s) with the propensity for expansion.[5] Hematoma location has not yet been included as a potential modifier in expansion prediction scores.[3,6,8] We defined location as the center of the hematoma, finding it to be a significant predictor of expansion in our dataset and improved the 3D-TBM model's performance. Visualized as a vector, the direction most discriminating expansion was oriented towards the thalamus, posterior limb of the internal capsule and atrium of the lateral ventricle. Our method for defining location affords advantages of precision and reproducibility. Our observations lend weight to the need for an improved understanding of the relationships between hematoma location, expansion, and neurological

outcome.

Artificial intelligence will play an increasingly important role in modeling medical information.[25] However, several limitations to current deep learning methods exist.[26-28] First, they frequently lack connection to an underlying physical process that can provide a scientific rationale for its use.[28,29] Second, they require large amounts of training data which can be unrealistic to obtain in a clinical setting.[30] Third, they lack robustness to adversarial information as small variations in the data can cause them to make confident but erroneous predictions.[29] Transport-based mathematical representation techniques for biomedical images can overcome these challenges.[11-13] Because medical imaging modalities generate images from physical phenomena, they can be modeled using continuum mechanics.[12,13] By considering normalized intensity values as relative measurements of blood density, we applied our 3D-TBM framework to map each pixel intensity within a hematoma.[13,16,17] Our method offers several advantages. First, preserving the information content of each image within a biologically meaningful representation allows the difference between two hematoma images to be quantified, thereby permitting visualization of changes in morphology and location.[12] Second, within a limited size dataset, it can detect and interpret discriminating information between hematomas which do and do not expand.[16,17] Third, it is robust to variations in imaging protocols and resolutions, enabling comparisons across a range of CT acquisition methods.[13]

This study developed and internally validated a novel methodology for prediction of hematoma expansion using NCCT images. Our 3D-TBM model's contributions are: (1) it outperformed clinician-based methods for predicting hematoma expansion, (2) it is fully automated and (3) it

biologically modelled hematoma expansion, enabling discovery of mechanisms driving the disease pathophysiology. Our method was limited by the small sample size of 170 patients and its retrospective design. The limited intensity information on NCCT and the small number of patients who experienced hematoma expansion (n=56) in our dataset are likely to have affected the predictive strength of the model. Because the number of clinical variables included was limited by the total number of patients in the dataset and risk of overfitting, the relationship between NCCT and clinical predictors of hematoma expansion warrants further investigation. Furthermore, because our expansion definition was not based on clinical outcome, we expect future studies to investigate the effect of TBM-based hematoma expansion prediction on neurological outcome. The 3D-TBM model utilized input of manually segmented images, which can be time consuming and impractical in the clinical setting. Future studies may take advantage of fully automated hematoma segmentation methods, which are in the process of validation.[31,32] As a promising preclinical study, our 3D-TBM model motivates external validation studies to define its translation potential to the clinical setting.

Conclusions

Using 3D TBM, we present a fully automated method for predicting hematoma expansion from NCCT in ICH patients. Our model outperformed current clinician based NCCT scores for predicting hematoma expansion, is mathematically reproducible, and affords insight into the image features used for its predictions. This may permit early selection of ICH patients for therapeutic intervention. A larger external validation study is underway.

Data availability

Data used for his manuscript is available from the corresponding author upon reasonable request.

Figure Legends

Figure 1. Example of the preprocessing protocol. **(A)** All NCCT scans were skull stripped and registered to a population-based high resolution NCCT template with dimensions of 256 x 256 x 256 and voxel spacings of 1 x 1 x 1mm. **(B)** example registered NCCT axial slice at presentation and **(C)** 24 hours in a patient with hematoma expansion. **(F)** the corresponding segmented and normalized hematoma image at presentation **(G)** and 24-hours for the same patient. **(D)** example registered NCCT axial slice at presentation **(E)** and 24 hours in a patient without hematoma expansion. **(H)** The corresponding normalized hematoma image at presentation **(I)** and 24-hours in the same patient. In examples of segmented presentation non-contrast computed tomography (NCCT) hematoma images separated into groups of **(J)** hematoma expansion (≥ 6mL hematoma volume increase at the 24 hour interval NCCT scan) and **(K)** no hematoma expansion (<6mL hematoma volume increase at the 24 hour interval NCCT scan), a visually discernible difference was not identified between the two groups. Abbreviations: NCCT = non-contrast computed tomography.

Figure 2. Results of the TBM model adjusted for location and clinical information in predicting 24-hour hematoma expansion from the testing dataset. **(A)** Mean probability distributions of the hematoma image features in the testing dataset projected onto the most discriminant direction w_0 in transport space showing the degree of separation between the expansion (red) and no expansion (blue) groups by the learned pLDA classifier boundary. **(B)** AUROC analyses and corresponding 95% confidence intervals of the performance of the pLDA classifier in the testing dataset for **(C)** Inverse transformations of three two-dimensional axial slice examples of the hematoma morphometric features found by the model to be associated with increasing likelihood of expansion, shown from left to right of the *x*-axis **(D)** Inverse transformations of the hematoma morphometric features overlaid onto the axial NCCT scan *least* associated with expansion, left, and *most* associated with expansion, right. Abbreviations: NCCT = non-contrast computed tomography, TBM = transport-based morphometry, AUROC = area under

the receiver operator curve, pLDA = penalized linear discriminant analysis, σ = standard deviation of the pixel intensity distribution along w_0.

Figure 3. Results of the TBM model adjusted for location and clinical information in predicting 24-hour hematoma volume from the testing dataset. **(A)** Scatter plots showing the relationship between the hematoma image features in the testing dataset projected onto the most correlated direction w_{corr} in transport space and change in hematoma volume from the presentation to the 24-hour NCCT scan. **(B)** Inverse transformations of three two-dimensional axial slice examples of the hematoma morphometric features found by the model to be associated with increasing growth, shown from left to right of the *x*-axis **(C)** Inverse transformations of the hematoma morphometric features overlaid onto the axial NCCT scan associated with *least* growth, left, and *most* growth, right. Abbreviations: NCCT = non-contrast computed tomography, TBM = transport-based morphometry, CC = correlation co-efficient σ = standard deviation of the pixel intensity distribution along w_{corr}.

Figure 4. Independent effects of hematoma location as a predictor of 24-hour hematoma expansion. Two-dimensional examples of inverse transformations overlaid onto NCCT scans in the axial (top row), sagittal (second row) and coronal (third row) planes showing from left to right of the *x*-axis the hematoma morphometric features and location direction found by the TBM model to be associated with increasing likelihood of expansion. Abbreviations: NCCT = non-contrast computed tomography, TBM = transport-based morphometry, σ = standard deviation of the pixel intensity distribution along w_0.

Figure 5. Comparisons of the performance between existing NCCT hematoma expansion prediction scores and the final TBM model adjusted for location and clinical information. AUROC analyses and corresponding 95% confidence intervals in the (A) testing dataset and (B) training dataset. Hematoma expansion was defined as ≥ 6mL hematoma volume increase from the presentation to the 24±6 hour NCCT scan. Abbreviations: AUROC = Area Under the Receiver Operator Curve, ROC = Receiver Operator Curve, TBM = transport-based morphometry, NCCT = non-contrast computed tomography, Heavn = Heavn score, Brain = Brain score, NAG = NAG scale, PT = 10-point score, BAT = BAT score, TBM = transport-based

morphometry.

Tables

	Expansion (n=56)	No expansion (n=114)	p-value
Demographics			
Age, years, mean ± S.D	66.16 ± 11.89	63.06 ± 12.64	0.127
Female, n (%)	19 (33.9)	45 (39.5)	0.483
Biochemistry			
INR*, mean ± S.D.	1.07 ± 0.26	1.10 ± 0.19	0.564
Clinical parameters			
SBP*, mean mmHg ± S.D.	185 ± 30	181 ± 28	0.464
Radiographic parameters			
Time from symptom onset to NCCT, mean min ± S.D.	104.13 ± 37.7	113.58 ± 41.3	0.151
Hematoma growth rate, mean mL/min ± S.D.	0.426 ± 0.279	0.281 ± 0.375	**0.012**
IVH score, median [IQR]	0 [0-2]	0 [0-1]	0.405

Table 1: Comparison of demographic and clinical information between the expansion and no expansion groups. Abbreviations: INR = international normalized ratio, S.D. = standard deviation, n = number, IVH = intraventricular hemorrhage, NCCT = non-contrast computed tomography, IQR = interquartile range. * on admission.

References

1. Dowlatshahi D, Demchuk AM, Flaherty ML, Ali M, Lyden PL, Smith EE. Defining hematoma expansion in intracerebral hemorrhage: relationship with patient outcomes. *Neurology*. Apr 5 2011;76(14):1238-44. doi:10.1212/WNL.0b013e3182143317
2. Morotti A, Boulouis G, Dowlatshahi D, et al. Intracerebral haemorrhage expansion: definitions, predictors, and prevention. *Lancet Neurol*. Feb 2023;22(2):159-171. doi:10.1016/s1474-4422(22)00338-6
3. Brott T, Broderick J, Kothari R, et al. Early hemorrhage growth in patients with intracerebral hemorrhage. *Stroke*. Jan 1997;28(1):1-5. doi:10.1161/01.str.28.1.1
4. Mayer SA, Frontera JA, Jankowitz B, et al. Recommended Primary Outcomes for Clinical Trials Evaluating Hemostatic Agents in Patients With Intracranial Hemorrhage: A Consensus Statement. *JAMA Netw Open*. Sep 1 2021;4(9):e2123629. doi:10.1001/jamanetworkopen.2021.23629
5. Hemphill JC, 3rd. Hematoma Expansion in ICH: Targeting Epidemiology or Biology? *Neurocrit Care*. Aug 2019;31(1):9-10. doi:10.1007/s12028-019-00752-1
6. Morotti A, Dowlatshahi D, Boulouis G, et al. Predicting Intracerebral Hemorrhage Expansion With Noncontrast Computed Tomography: The BAT Score. *Stroke*. May 2018;49(5):1163-1169. doi:10.1161/strokeaha.117.020138
7. Brouwers HB, Chang Y, Falcone GJ, et al. Predicting hematoma expansion after primary intracerebral hemorrhage. *JAMA Neurol*. Feb 2014;71(2):158-64. doi:10.1001/jamaneurol.2013.5433
8. Yogendrakumar V, Moores M, Sikora L, et al. Evaluating Hematoma Expansion Scores in Acute Spontaneous Intracerebral Hemorrhage: A Systematic Scoping Review. *Stroke*. Apr 2020;51(4):1305-1308. doi:10.1161/strokeaha.119.028574
9. Naidech AM, Grotta J, Elm J, et al. Recombinant factor VIIa for hemorrhagic stroke treatment at earliest possible time (FASTEST): Protocol for a phase III, double-blind, randomized, placebo-controlled trial. *Int J Stroke*. Aug 2022;17(7):806-809. doi:10.1177/17474930211042700
10. Pradilla G, Ratcliff JJ, Hall AJ, et al. Trial of Early Minimally Invasive Removal of Intracerebral Hemorrhage. *N Engl J Med*. Apr 11 2024;390(14):1277-1289. doi:10.1056/NEJMoa2308440
11. Shifat ERM, Yin X, Rubaiyat AHM, et al. Radon Cumulative Distribution Transform Subspace Modeling for Image Classification. *J Math Imaging Vis*. Nov 2021;63(9):1185-1203. doi:10.1007/s10851-021-01052-0
12. Kolouri S, Park S, Thorpe M, Slepčev D, Rohde GK. Optimal Mass Transport: Signal processing and machine-learning applications. *IEEE Signal Process Mag*. Jul 2017;34(4):43-59. doi:10.1109/msp.2017.2695801
13. Basu S, Kolouri S, Rohde GK. Detecting and visualizing cell phenotype differences from microscopy images using transport-based morphometry. *Proc Natl Acad Sci U S A*. Mar 4 2014;111(9):3448-53. doi:10.1073/pnas.1319779111
14. Wang W, Slepčev D, Basu S, Ozolek JA, Rohde GK. A linear optimal transportation framework for quantifying and visualizing variations in sets of images. *Int J Comput Vis*. Jan 1 2013;101(2):254-269. doi:10.1007/s11263-012-0566-z
15. Kolouri S, Tosun AB, Ozolek JA, Rohde GK. A continuous linear optimal transport approach for pattern analysis in image datasets. *Pattern Recognit*. Mar 1 2016;51:453-462. doi:10.1016/j.patcog.2015.09.019
16. Kundu S, Ashinsky BG, Bouhrara M, et al. Enabling early detection of osteoarthritis from presymptomatic cartilage texture maps via transport-based learning. *Proc Natl Acad Sci U S A*. Oct 6 2020;117(40):24709-24719. doi:10.1073/pnas.1917405117
17. Kundu S, Kolouri S, Erickson KI, Kramer AF, McAuley E, Rohde GK. Discovery and visualization of structural biomarkers from MRI using transport-based morphometry. *NeuroImage*. 2018;167:256-275.
18. Ali M, Bath P, Brady M, et al. Development, expansion, and use of a stroke clinical trials resource for novel exploratory analyses. *Int J Stroke*. Feb 2012;7(2):133-8. doi:10.1111/j.1747-4949.2011.00735.x
19. Huttner HB, Gerner ST, Kuramatsu JB, et al. Hematoma Expansion and Clinical Outcomes in Patients With Factor-Xa Inhibitor-Related Atraumatic Intracerebral Hemorrhage Treated Within the ANNEXA-4 Trial Versus Real-World Usual Care. *Stroke*. Feb 2022;53(2):532-543. doi:10.1161/strokeaha.121.034572
20. Morotti A, Boulouis G, Charidimou A, et al. Hematoma Expansion in Intracerebral Hemorrhage With Unclear Onset. *Neurology*. May 11 2021;96(19):e2363-e2371. doi:10.1212/wnl.0000000000011895
21. Wang X, Arima H, Al-Shahi Salman R, et al. Clinical prediction algorithm (BRAIN) to determine risk of hematoma growth in acute intracerebral hemorrhage. *Stroke*. Feb 2015;46(2):376-81.

doi:10.1161/strokeaha.114.006910
22. Miyahara M, Noda R, Yamaguchi S, et al. New Prediction Score for Hematoma Expansion and Neurological Deterioration after Spontaneous Intracerebral Hemorrhage: A Hospital-Based Retrospective Cohort Study. *J Stroke Cerebrovasc Dis*. Sep 2018;27(9):2543-2550. doi:10.1016/j.jstrokecerebrovasdis.2018.05.018
23. Sakuta K, Sato T, Komatsu T, et al. The NAG scale: Noble Predictive Scale for Hematoma Expansion in Intracerebral Hemorrhage. *J Stroke Cerebrovasc Dis*. Oct 2018;27(10):2606-2612. doi:10.1016/j.jstrokecerebrovasdis.2018.05.020
24. Fu J, Hu S, Yang M, et al. A Novel 10-Point Score System to Predict Early Hematoma Growth in Patients With Spontaneous Intracerebral Hemorrhage. *Front Neurol*. 2019;10:1417. doi:10.3389/fneur.2019.01417
25. Wang F, Casalino LP, Khullar D. Deep learning in medicine—promise, progress, and challenges. *JAMA internal medicine*. 2019;179(3):293-294.
26. Stead WW. Clinical Implications and Challenges of Artificial Intelligence and Deep Learning. *Jama*. Sep 18 2018;320(11):1107-1108. doi:10.1001/jama.2018.11029
27. Kundu S. Measuring trustworthiness is crucial for medical AI tools. *Nat Hum Behav*. Nov 2023;7(11):1812-1813. doi:10.1038/s41562-023-01711-9
28. Kundu S. AI in medicine must be explainable. *Nat Med*. Aug 2021;27(8):1328. doi:10.1038/s41591-021-01461-z
29. Hosseini H, Xiao B, Jaiswal M, Poovendran R. On the limitation of convolutional neural networks in recognizing negative images. IEEE; 2017:352-358.
30. Beam AL, Manrai AK, Ghassemi M. Challenges to the reproducibility of machine learning models in health care. *Jama*. 2020;323(4):305-306.
31. Ironside N, Patrie J, Ng S, et al. Quantification of hematoma and perihematomal edema volumes in intracerebral hemorrhage study: Design considerations in an artificial intelligence validation (QUANTUM) study. *Clinical Trials*. 2022;19(5):534-544.
32. Ironside N, Chen CJ, Mutasa S, et al. Fully Automated Segmentation Algorithm for Hematoma Volumetric Analysis in Spontaneous Intracerebral Hemorrhage. *Stroke*. Dec 2019;50(12):3416-3423. doi:10.1161/strokeaha.119.026561
33. Al-Shahi Salman R, Frantzias J, Lee RJ, et al. Absolute risk and predictors of the growth of acute spontaneous intracerebral haemorrhage: a systematic review and meta-analysis of individual patient data. *Lancet Neurol*. Oct 2018;17(10):885-894. doi:10.1016/s1474-4422(18)30253-9
34. Monge G. Mémoire sur la théorie des déblais et des remblais. *Mem Math Phys Acad Royale Sci*. 1781:666-704.
35. Rohde GK. PyTransKit. https://github.com/rohdelab/PyTransKit

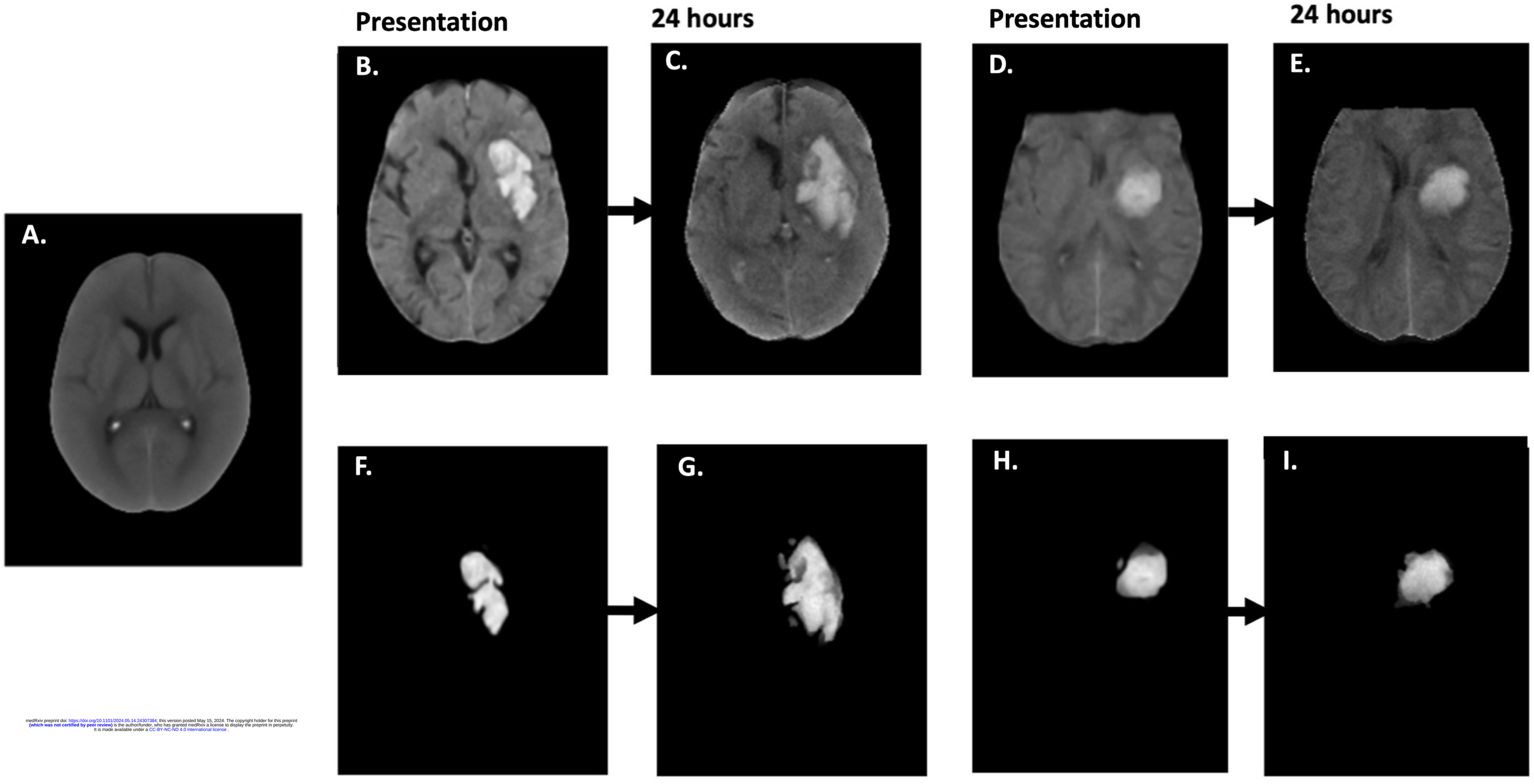

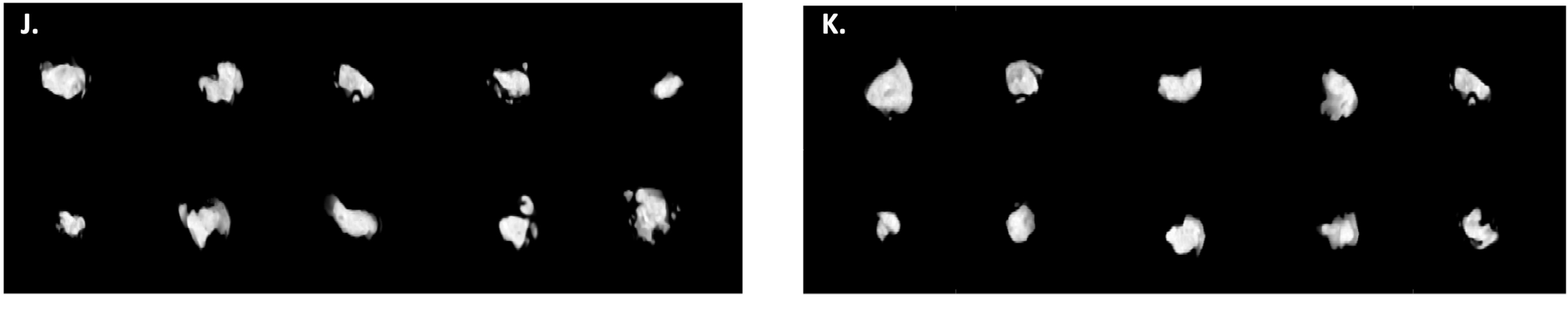

A.

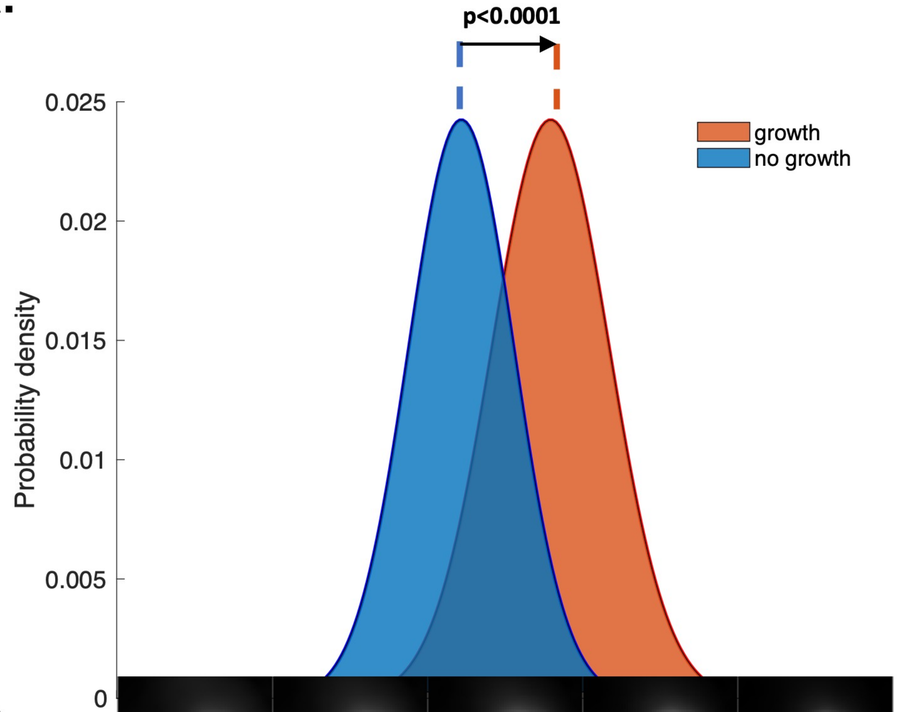
p<0.0001
growth
no growth
Probability density
0.025
0.02
0.015
0.01
0.005
0

B.

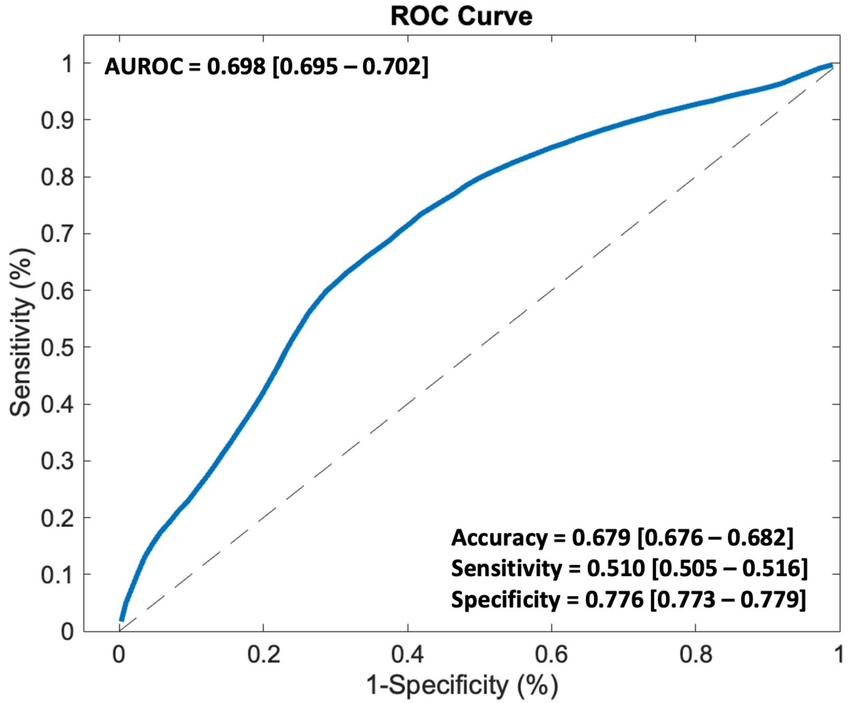
ROC Curve
AUROC = 0.698 [0.695 – 0.702]
Accuracy = 0.679 [0.676 – 0.682]
Sensitivity = 0.510 [0.505 – 0.516]
Specificity = 0.776 [0.773 – 0.779]
Sensitivity (%)
1-Specificity (%)

C.

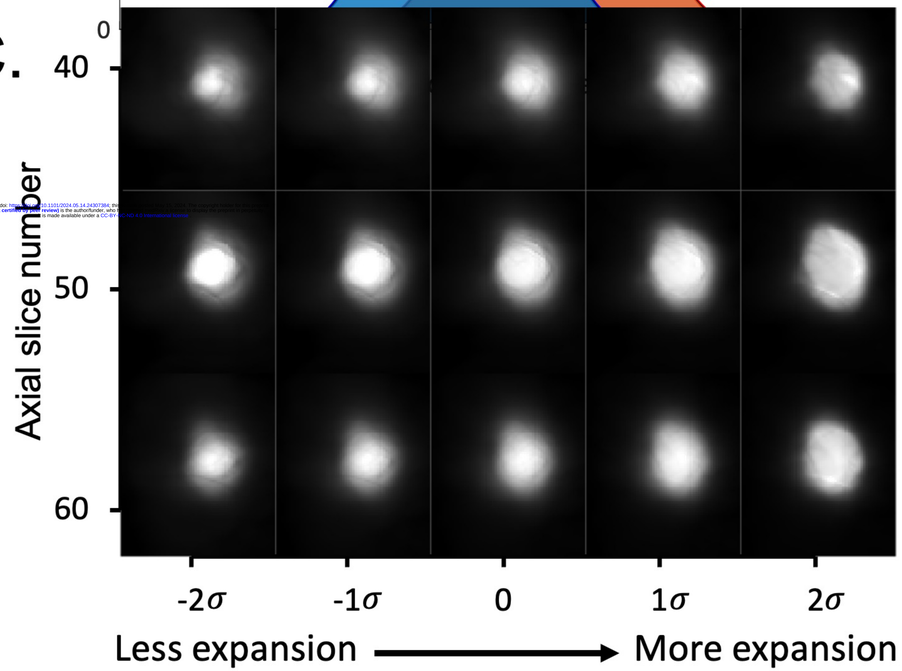
Axial slice number
40
50
60
-2σ
-1σ
0
1σ
2σ
Less expansion
More expansion

D.

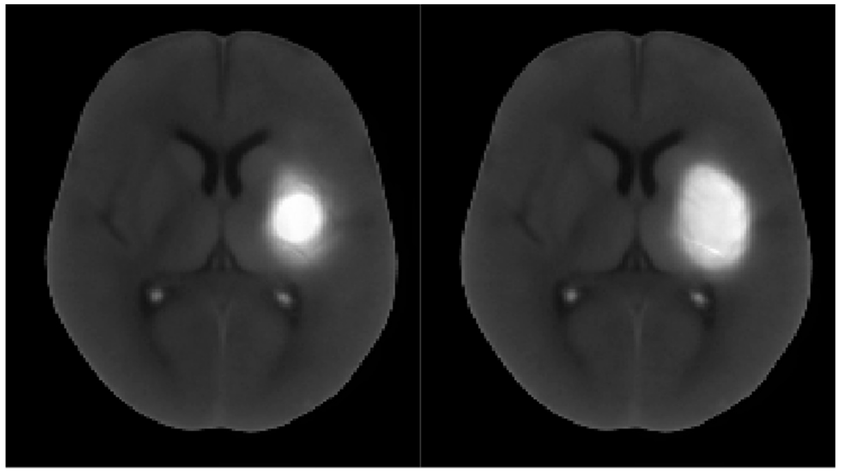
−2σ
2σ
Less expansion
More expansion

A.

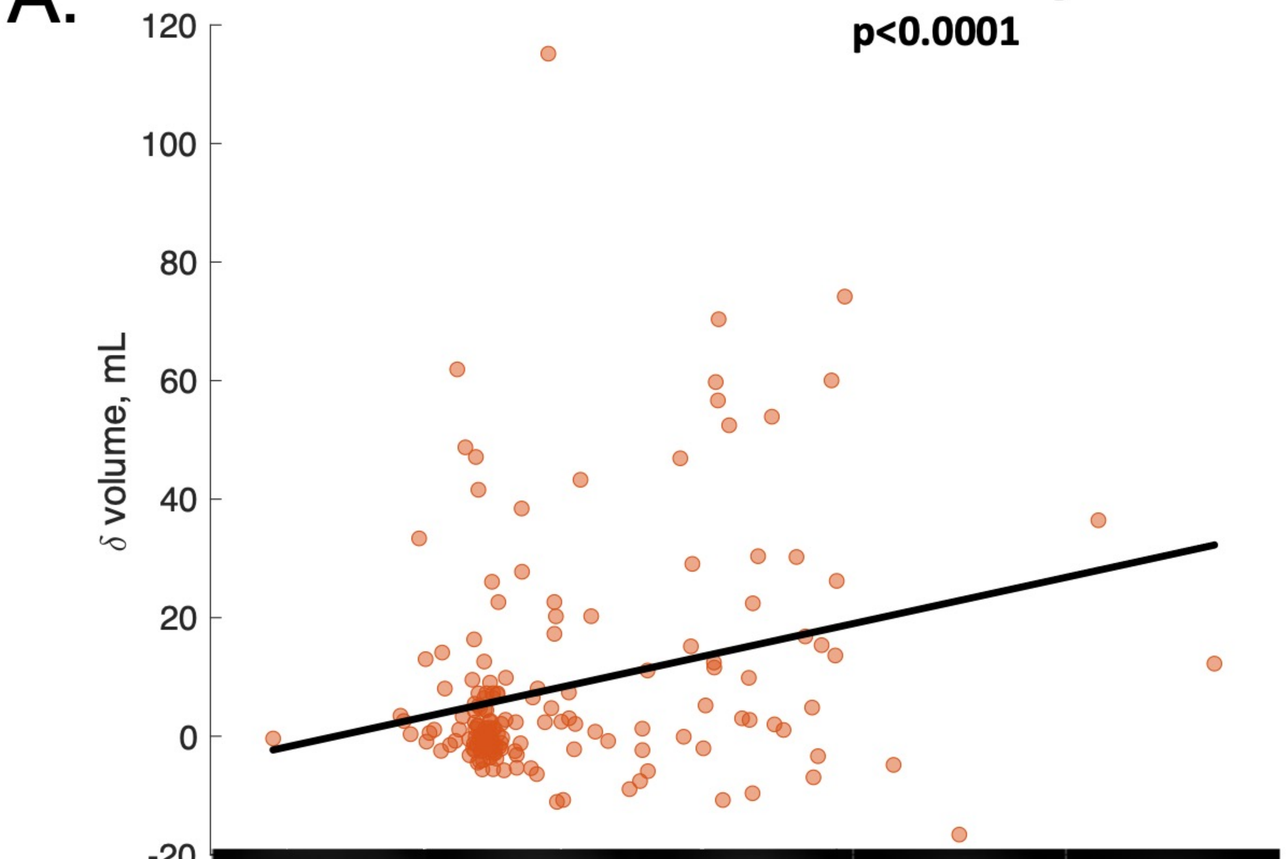

B.

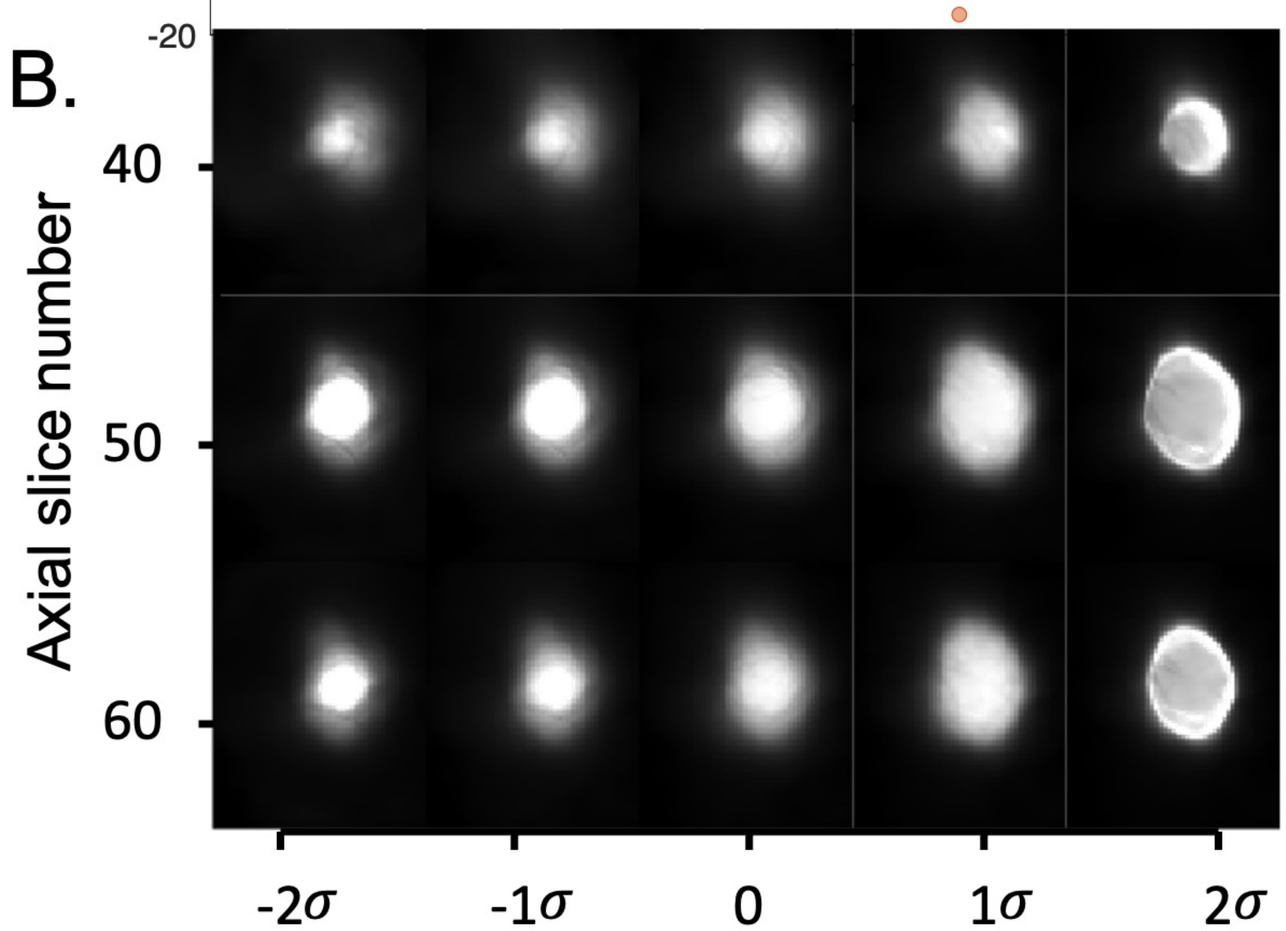

C.

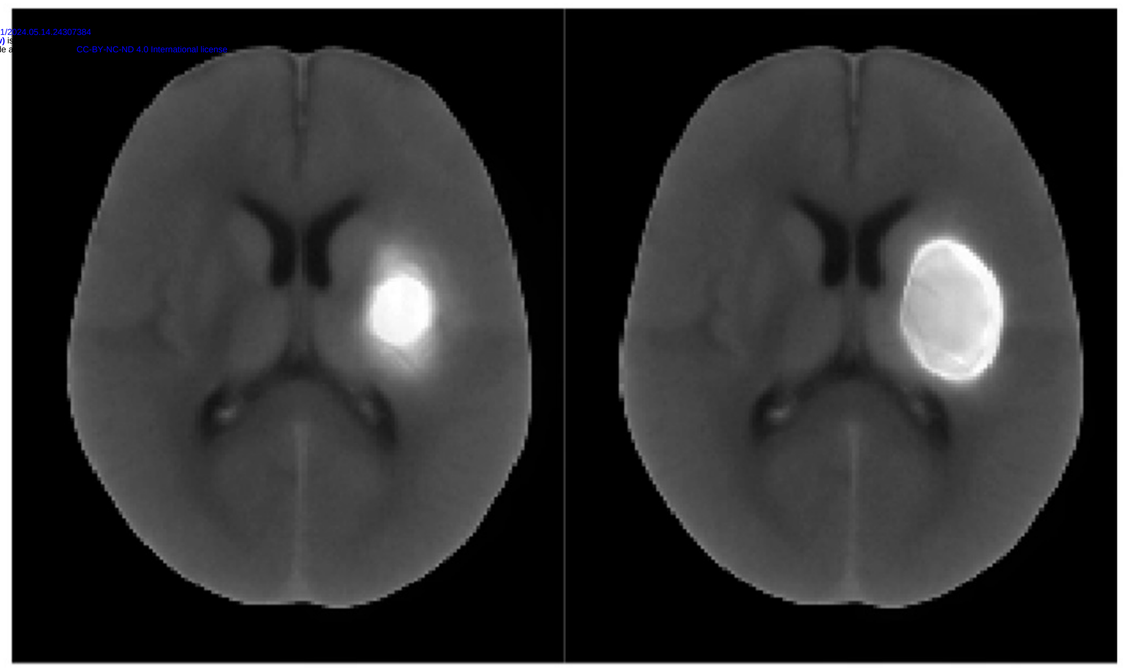

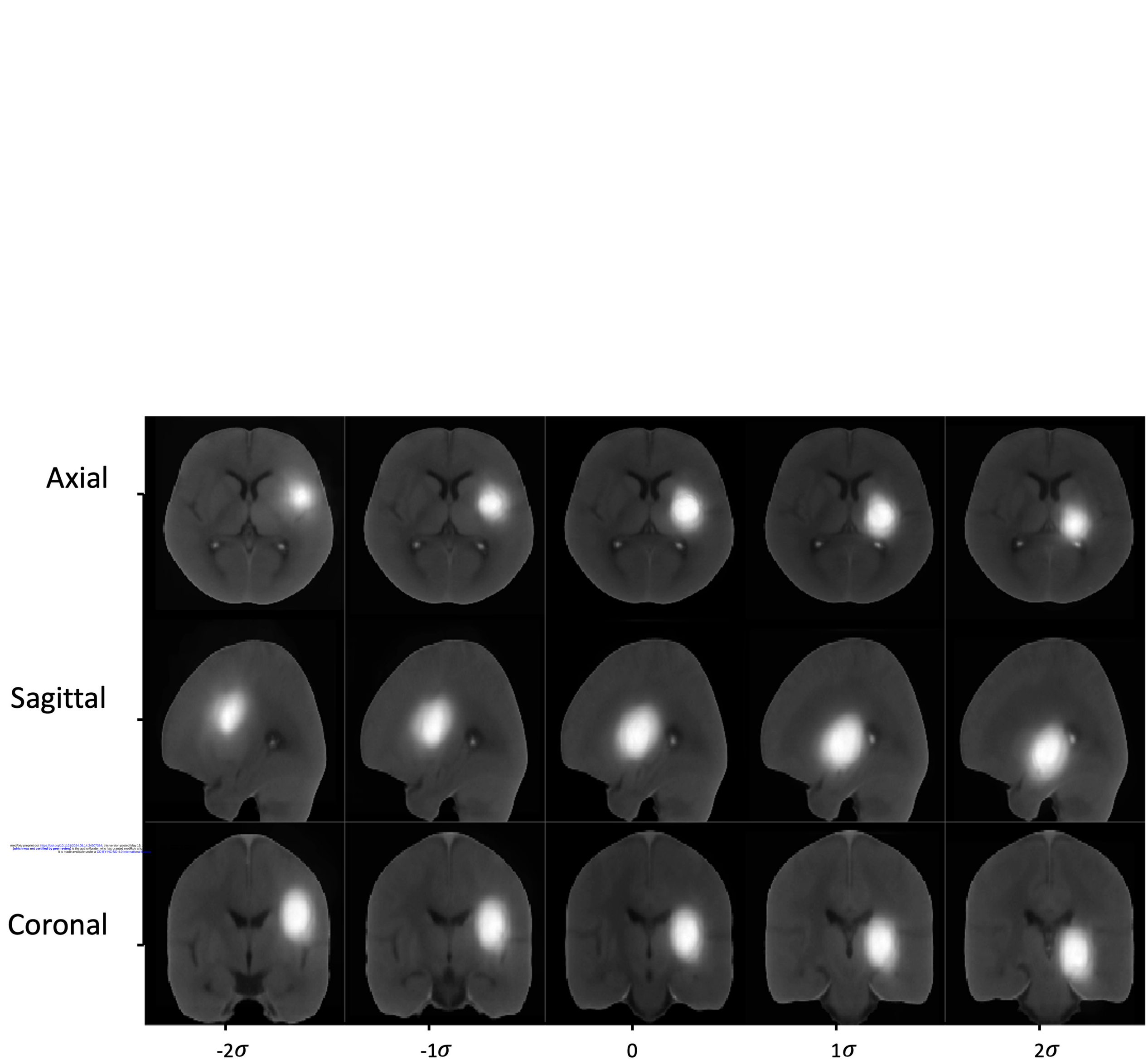

A.

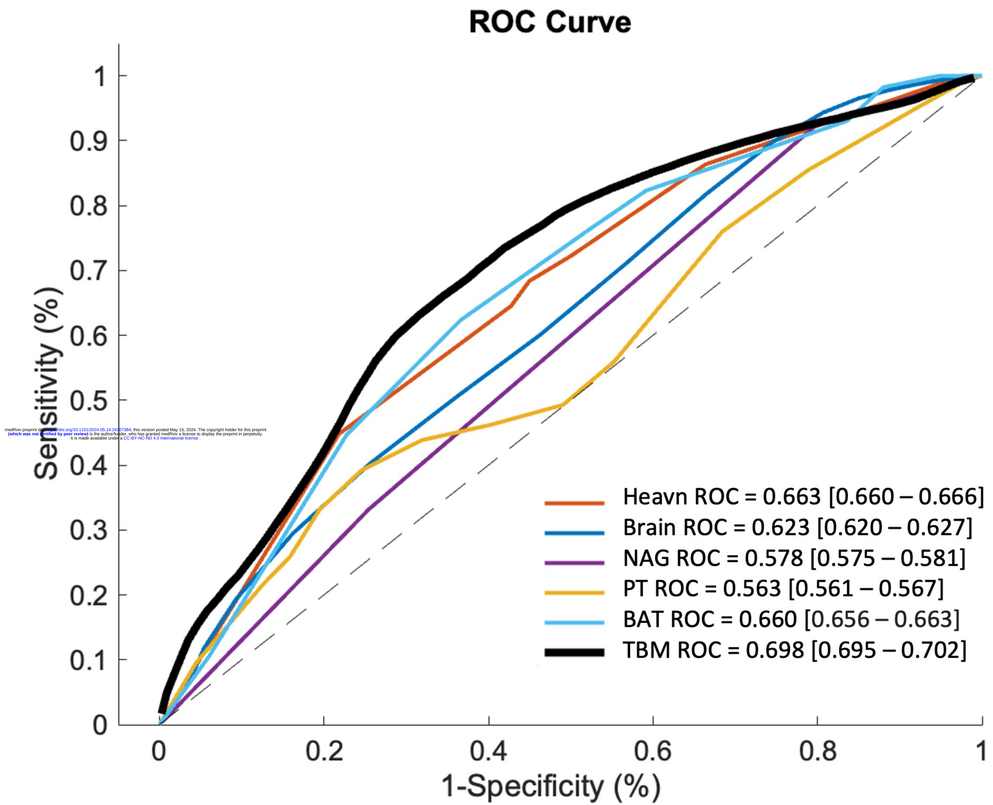
ROC Curve
Sensitivity (%)
1-Specificity (%)
0
0.1
0.2
0.3
0.4
0.5
0.6
0.7
0.8
0.9
1
Heavn ROC = 0.663 [0.660 – 0.666]
Brain ROC = 0.623 [0.620 – 0.627]
NAG ROC = 0.578 [0.575 – 0.581]
PT ROC = 0.563 [0.561 – 0.567]
BAT ROC = 0.660 [0.656 – 0.663]
TBM ROC = 0.698 [0.695 – 0.702]

B.

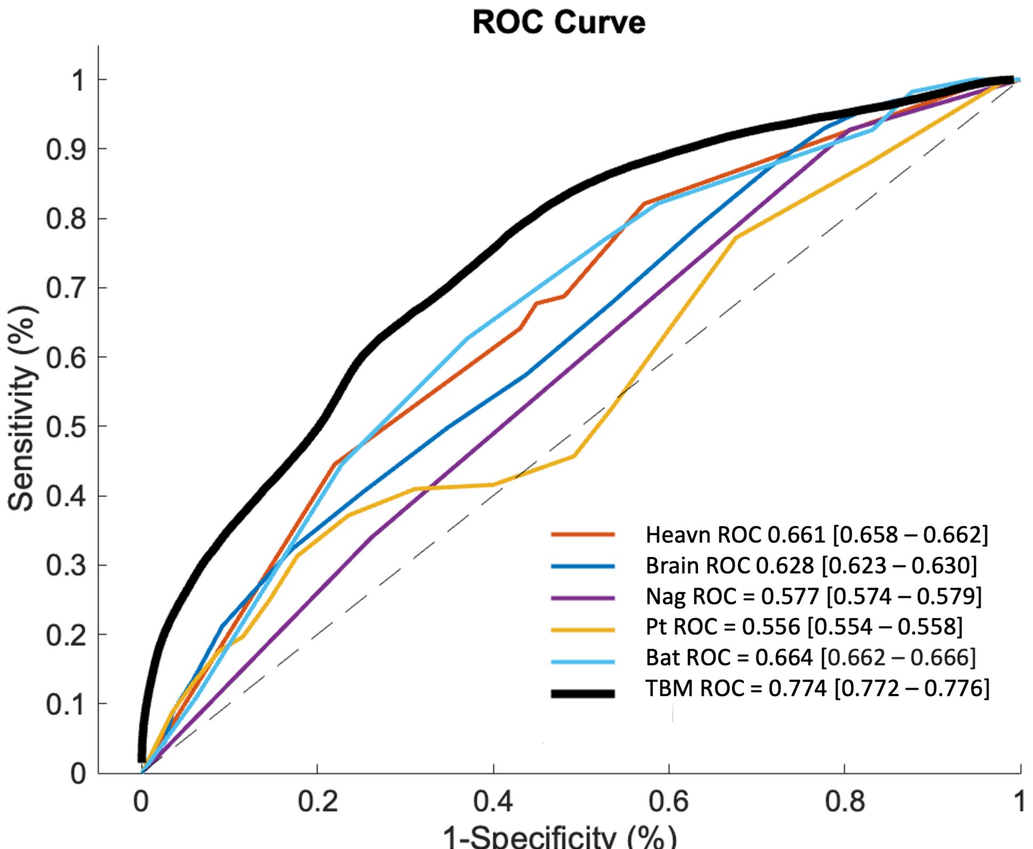
ROC Curve
Sensitivity (%)
1-Specificity (%)
0
0.1
0.2
0.3
0.4
0.5
0.6
0.7
0.8
0.9
1
Heavn ROC 0.661 [0.658 – 0.662]
Brain ROC 0.628 [0.623 – 0.630]
Nag ROC = 0.577 [0.574 – 0.579]
Pt ROC = 0.556 [0.554 – 0.558]
Bat ROC = 0.664 [0.662 – 0.666]
TBM ROC = 0.774 [0.772 – 0.776]